Impedance matching for an asymmetric dielectric barrier discharge plasma actuator

Kunwar Pal Singh and Subrata Roy[a)]
Computational Plasma Dynamics Laboratory and Test Facility, Department of Mechanical and Aerospace Engineering, University of Florida, Gainesville, Florida 32611

(Received 8 April 2007; accepted 30 July 2007; published online 23 August 2007)

A typical dielectric barrier discharge plasma actuator requires a power supply capable of delivering power at a frequency range of several kilohertz and a rms voltage up to 20 kV. An impedance mismatch resulting from the absence of a matching network causes a large reflected power from the plasma actuator back to the power supply. This does not contribute to plasma formation and requires an expensive over-rated power supply. The authors suggest an impedance matching network for a realistic asymmetric dielectric barrier discharge plasma actuator with a virtual electrode. © *2007 American Institute of Physics*. [DOI: 10.1063/1.2773932]

Active control of air flow using surface plasma actuators has emerged in recent years. Such control involves modifying air flow pattern with the help of electrical discharge for increasing the aerodynamic efficiency. Plasma actuators use reasonably small external power and have the advantage of being accurately controllable, i.e., they can be turned on and off with near instantaneous fluid response.[1] A plasma actuator consists of establishing an electrical discharge along a dielectric surface in order to add momentum to the surrounding air close to the wall.[2,3] A direct current corona discharge and a dielectric barrier discharge (DBD) have been demonstrated for flow modification along flat plates[4] and for stall control over airfoils.[5] The weakly ionized gas in such a discharge is called nonthermal plasmas due to its nonthermodynamic equilibrium state, where the ion and gas temperature is much lower than that of the electrons. The mechanisms and responses of a single dielectric barrier plasma actuator have been studied by Enloe *et al.*[6] and Van Dyken *et al.*[7] Also, plasma characterization of a 1 atm uniform barrier discharge has been documented by Borghi *et al.*[8]

The DBD plasma actuator produces an electrodynamic body force which results in modification of the surrounding air flow. The plasma actuator is an inefficient device as its impedance is not typically matched to the power supply. Thus optimization of impedance of the load experienced by the power supply is necessary such that these actuators can perform at low power while delivering maximum energy to the plasma.[9] In modeling the plasma actuator, typically an *RC* circuit is used. The resistive element in the circuit is the plasma formed due to ionization of the air. The DBD actuator can operate in a wide range of geometrical configurations. It requires a power supply capable of delivering power at a frequency range of several kilohertz and a rms voltage of up to 20 kV. Such actuator is mainly a capacitive load seen by the power supply and the secondary side of the transformer. The plasma energized can be modeled as a capacitor in parallel with a resistor and inductor. The transformer converts the low voltage output of the power supply to a high voltage for plasma formation. The capacitive plasma actuator can reflect a large part of input power back to the power supply, and only a small part of the power supply output power is delivered to the plasma. The reflected power mandates an expensive over-rated power supply. Thus, the load for the power supply, seen by its output terminals, is highly reactive. The equivalent impedance of the plasma is strongly dependent on the power dissipated in it.[10,11] For optimum performance, an impedance matching circuit must be inserted between the power supply and the plasma actuator in order to operate an actuator efficiently.[12,13] The impedance matching to the load can be optimized by changing the electrical parameters of the matching network.

We study impedance matching for a dielectric barrier discharge plasma actuator in this letter. The impedance matching problem has not been studied for an asymmetric dielectric barrier plasma actuator by other authors. For such asymmetric electrode configuration one needs to take into account the virtual electrode due to charge deposition over the dielectric surface in the vicinity of the grounded electrode.[14,15] The equivalent impedance of the plasma actuator has been found to be highly capacitive. We study how the use of an *LCR* circuit can reduce the capacitive reactance substantially. We also consider the use of a suitable inductor to facilitate impedance matching.

A schematic of a plasma actuator is shown in Fig. 1 with different resistances, capacitances, and inductances. Based on the physics of the problem, we have imposed a virtual electrode parallel to the grounded electrode over the dielectric surface.[14,15] There are two capacitive components: one between the rf electrode and grounded electrode (C_d) and another between the virtual electrode and grounded electrode (C_{dv}). The equivalent circuit diagram of the plasma actuator is shown in Fig. 2. The dielectric barrier discharge plasma actuator is essentially a capacitor (C_p) and an inductor (L_p) in parallel, one resistor (r_p) and one capacitor (C_{dv}) in series

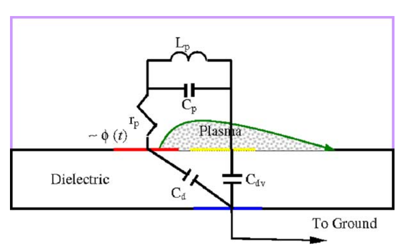

FIG. 1. (Color online) Schematic of an asymmetric single dielectric barrier plasma actuator with various resistances and capacitances.

[a)]Author to whom correspondence should be addressed; electronic mail: roy@ufl.edu

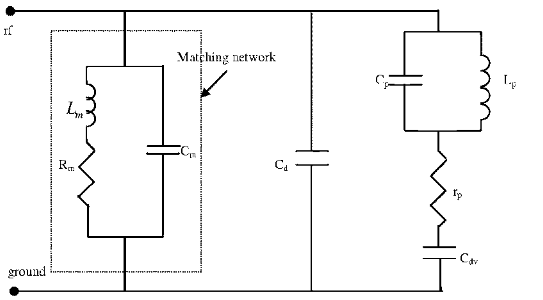

FIG. 2. Equivalent circuit diagram of an asymmetric single dielectric barrier plasma actuator with an impedance matching network. The various capacitances and inductances are C_p=1 nF, L_p=1 pH, C_{dv}=1 pF, and C_d=1 pF.

to this, and one capacitor (C_d) parallel to the full circuit. When the plasma is energized, a resistive component (R_p) that is responsible for the power dissipation in the plasma is added to the plasma capacitor (C_p) and the plasma inductor (L_p). We use an *LCR* circuit in parallel to the grounded and powered electrodes for impedance matching. This model is sufficient for impedance matching between the power source and the plasma actuator. The plasma resistance is due to the charge transport in plasma. The electron oscillation between two collisions gives rise to an inductive component of plasma. Also plasma capacitance forms due to the existence of sheath regions.

In Fig. 2, the plasma capacitor (C_p) and the plasma inductor (L_p) are parallel to each other with an equivalent reactance given by $(-L_p/C_p)/(L_p\omega-1/\omega C_p)$, where ω is the angular frequency of the applied rf voltage. The plasma resistance r_p and capacitance C_{dv} between the virtual and grounded electrodes are in series to the above reactance. The equivalent resistance for this part of the circuit is r_p and the reactance is $X_1=(-L_p/C_p)/(L_p\omega-1/\omega C_p)-1/C_{dv}\omega$.

The reactance associated with the capacitance between the rf electrode and grounded electrode (C_d) is given by $X_2=-1/C_d\omega$. This is parallel to the impedance given by X_1. Based on the circuit, the equivalent resistance and equivalent reactance of the plasma actuator in Figs. 1 and 2 are

$$R_p=\frac{X_2 r_p(X_1+X_2)-X_1X_2r_p}{r_p^2+(X_1+X_2)^2}, \quad (1)$$

$$X_p=\frac{X_2 r_p^2+X_1X_2(X_1+X_2)}{r_p^2+(X_1+X_2)^2}, \quad (2)$$

respectively. For impedance matching we use the matching network shown in Fig. 2. The equivalent resistance and reactance of the matching network are given by following equations:

$$R_{mq}=\frac{L_mR_m/C_m-(L_m\omega-1/C_m\omega)R_m/C_m\omega}{R_m^2+(L_m\omega-1/C_m\omega)^2}, \quad (3)$$

$$X_{mq}=\frac{-R_m^2/C_m\omega-L_m/C_m(L_m\omega-1/C_m\omega)}{R_m^2+(L_m\omega-1/C_m\omega)^2}. \quad (4)$$

The impedance is matched when the resistances of the power supply and the actuator device are the same and the reactances are complex conjugate of each other. The equivalent impedance of the plasma actuator along with the matching network is given by the following relations:

$$R_{\rm eq}=\frac{(X_pR_{mq}+X_{mq}R_p)(X_p+X_{mq})+(R_pR_{mq}-X_pX_{mq})(R_p+R_{mq})}{(R_p+R_{mq})^2+(X_p+X_{mq})^2}, \quad (5)$$

$$X_{\rm eq}=\frac{(X_pR_{mq}+X_{mq}R_p)(R_p+R_{mq})-(R_pR_{mq}-X_pX_{mq})(X_p+X_{mq})}{(R_p+R_{mq})^2+(X_p+X_{mq})^2}. \quad (6)$$

We have used the following values of various capacitances and inductances to calculate the impedance of the equivalent circuit diagram:C_p=1 nF, L_p=1 pH, C_{dv}=1 pF, and C_d=1 pF.

Figure 3 shows the resistance and reactance of the plasma actuator given by Eqs. (1) and (2) as a function of angular frequency. No impedance matching network is used for the results of this figure. The plasma density depends on the geometry of the actuator and the amplitude of the rf voltage. The results are shown for three values of the plasma resistance, r_p=0.1, 1, and 10 Ω. The equivalent resistance of the plasma actuator decreases with frequency and is very low at high frequencies. The equivalent reactance of the plasma actuator is negative indicating that the reactive part is due to capacitance. The reactance is in the order of megaohm at kilohertz operating frequency ranges which causes an impedance mismatch between the plasma actuator and power supply resulting in high power loss. The capacitance between the rf electrode and grounded electrode, C_d, is responsible for this. The equivalent reactance is negative due to C_d. The value of the equivalent reactance decreases with frequency for a capacitor. The capacitive reactance may be compensated by adding one inductor in parallel to the actuator.

Figure 4(a) shows the resistance and reactance of the plasma actuator as given in Eqs. (5) and (6) as a function of angular frequency. We have used an inductor L_m=0.1 pH with R_m=0.1 Ω in parallel to the plasma actuator for partial impedance matching. The frequency range is in kilohertz. The equivalent resistance changes from megaohm in Fig. 3(a) to 0.1 Ω in this figure due to *LR* impedance matching network. The equivalent reactance is positive and extremely small (nanoohms) for kilohertz operating frequency ranges. The positive value of reactance indicates an inductive component of reactance. Since the value of reactance is extremely small and the value of the device resistance with the network is 0.1 Ω and is independent of radio frequency, the plasma actuator will operate very close to the impedance matching condition and there will be an optimum transfer of the energy. A power supply with very low internal resistance (~0.1 Ω) is needed in this configuration for maximum

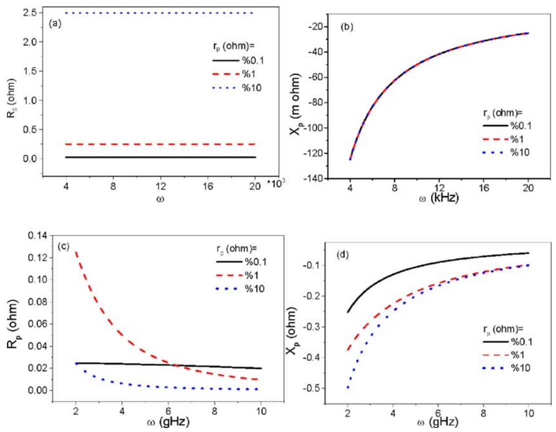

FIG. 3. (Color online) Plasma actuator as a function of angular frequency without any impedance matching network for different values of plasma resistance: (a) the resistance and (b) the reactance at low frequencies (kHz), and (c) the resistance and (d) the reactance at high frequencies (GHz).

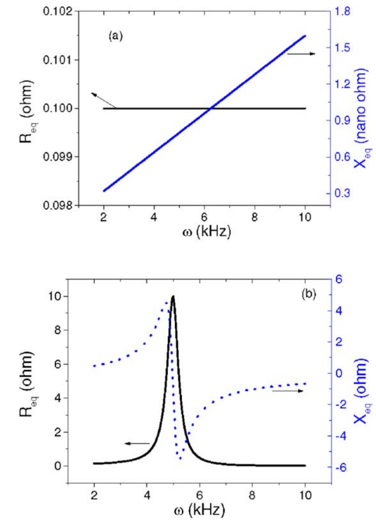

FIG. 4. (Color online) Resistance and reactance of the plasma actuator as a function of angular frequency for (a) only an *LR* matching network, $R_m = 0.1\ \Omega$ and $L_m = 0.1$ pH, (b) an *LCR* impedance matching network, $R_m = 0.1\ \Omega$, $L_m = 100\ \mu$H, and $C_m = 100\ \mu$F.

power transfer and even lower than this for a better efficiency. Figure 4(b) shows the equivalent resistance and reactance of the plasma actuator with an *LCR* impedance matching network as a function of angular frequency. Matching network parameters are $R_m = 0.1\ \Omega$, $L_m = 100\ \mu$H, and $C_m = 100\ \mu$F. The equivalent resistance peaks near the frequency related to impedance matching. The peak value of the equivalent resistance is 10 Ω. The equivalent reactance increases with radio frequency ω and peaks before the frequency related to impedance matching, then decreases upon reaching a negative peak. The value of reactance varies from nearly −5.0 to +5.0 Ω. The equivalent impedance is independent of plasma resistance r_p for both Figs. 4(a) and 4(b); hence, only one curve is shown.

In low-frequency systems, the reactance is small enough to be ignored and the maximum power transfer occurs when the resistance of the load is equal to the resistance of the source. Impedance matching is not always desirable. For example, if a source with low impedance is connected to a load with high impedance, then the power that can pass through the connection is limited by the higher impedance. However, in that case the voltage transfer is higher and less prone to reflection than when the impedances were matched. This maximum voltage connection is a common configuration called impedance bridging or voltage bridging. The condition of maximum power transfer does not result in maximum efficiency. If we define the efficiency η as the ratio of power dissipated by the load to power developed by the source, then

$$\eta = \frac{R_L}{R_L + R_S} = \frac{1}{1 + R_S/R_L}. \tag{7}$$

The efficiency is only 50% when maximum power transfer is achieved, but approaches 100% as the load resistance approaches infinity (though the total power level tends toward zero). When the load resistance is zero, all the power is consumed inside the source (the power dissipated in a short circuit is zero) so the efficiency is zero. As the equivalent resistance of the plasma actuator with a matching network is nearly 0.1 Ω in Fig. 4(a) and nearly 10 Ω (at matching frequency) in Fig. 4(b), the configuration in Fig. 4(a) may be less efficient than that in Fig. 4(b) if the power supply does not have a low resistance.

In conclusion, the load of the rf power supply, as seen by its output terminals, is highly reactive due to reactance of the capacitor between the rf electrode and grounded electrode. The reactance of the device keeps decreasing with frequency without any impedance matching. If we add a suitable matching network in parallel to the circuit, then maximum transfer of power occurs at kilohertz frequency range which may result in better efficiency as well.

This work was partially supported by AFOSR Grant No. FA9550-07-1-0131 under tasks monitored by Rhett Jefferies.

[1]A. Seifert, A. Darabi, and I. J. Wygnanski, J. Aircr. **33**, 691 (1993).
[2]J. R. Roth and Xin Dai, *44th AIAA Aerospace Sciences Meeting and Exhibit, Reno, NV, 9–12 January 2006* (AIAA, Washington, DC, 2002), Paper No. AIAA 2006-1203.
[3]O. K. Rediniotis, J. Ko, X. Yue, and A. J. Kurdilal, *37th Aerospace Sciences Meeting and Exhibit, Reno, NV, 12–15 January 1999* (AIAA, Washington, DC, 2002), Paper No. AIAA 99-l000.
[4]G. Artana, R. Sosa, E. Moreau, and G. Touchard, Exp. Fluids **35**, 580 (2003); S. Roy, K. P. Singh, and D. Gaitonde, Appl. Phys. Lett. **88**, 121501 (2006).
[5]S. El-Khabiry and G. Colver, Phys. Fluids **9**, 587 (1997); D. Gaitonde, M. Visbal, and S. Roy, Keynote Lecture FEDSM2006–98553, *ASME Joint U.S.-European Fluids Engineering Summer Meeting*, Miami, 2006.
[6]C. L. Enloe, T. E. McLaughlin, R. D. Vandyken, and K. D. Kachner, AIAA J. **42**, 595 (2004).
[7]R. Van Dyken, T. E. McLaughlin, and C. L. Enloe, *42nd Aerospace Sciences Meeting and Exhibit, Reno, NV, 5–8 January 2004* (AIAA, Washington, DC, 2002), Paper No. AIAA 2004-0846.
[8]C. A. Borghi, M. Carraro, and A. Cristofolini, *43rd AIAA Aerospace Sciences Meeting, Reno, NV, 10–13 January 2005* (AIAA, Washington, DC, 2002), Paper No. AIAA 2005-1179.
[9]Z. Chen, IEEE Trans. Plasma Sci. **30**, 5 (2002).
[10]M. M. Salem, J.-F. Loiseau, and B. Held, Eur. Phys. J.: Appl. Phys. **3**, 91 (1998); J. R. Roth, D. M. Sherman, R. B. Gadri, F. Karakaya, Z. Chen, T. C. Montie, K. Kelly-Wintenberg, and P. P.-Y. Tsai, IEEE Trans. Plasma Sci. **28**, 56 (2000).
[11]P. Colpo, R. Ernst, and J.-P. Keradec, Plasma Sources Sci. Technol. **8**, 587 (1999).
[12]M. G. Kong and Y. P. Lee, J. Appl. Phys. **90**, 3069 (2001).
[13]M. Watanabe, D. M. Shaw, G. J. Collins, and H. Sugai, J. Appl. Phys. **85**, 3428 (1999).
[14]S. Roy, Appl. Phys. Lett. **86**, 101502 (2005).
[15]G. I. Font, C. L. Enloe, T. E. McLaughlin, and D. Orlov, *45th AIAA Aerospace Sciences Meeting and Exhibit* (AIAA, Washington, DC, 2002).